International Atomic Energy Agency

INDC(IND)-041/LJ

INDC INTERNATIONAL NUCLEAR DATA COMMITTEE

BINARY AND TERTIARY NEUTRON INDUCED REACTION CROSS SECTIONS OF CHROMIUM AND IRON

S.B. Garg
Neutron Physics Division
Bhabha Atomic Research Centre
Trombay, Bombay 400 085, India

This work was performed under IAEA Research Contract 4391

January 1989

IAEA NUCLEAR DATA SECTION, WAGRAMERSTRASSE 5, A-1400 VIENNA

INDC(IND)-041/LJ

BINARY AND TERTIARY NEUTRON INDUCED REACTION CROSS SECTIONS OF CHROMIUM AND IRON

S.B. Garg
Neutron Physics Division
Bhabha Atomic Research Centre
Trombay, Bombay 400 085, India

This work was performed under IAEA Research Contract 4391

January 1989

Reproduced by the IAEA in Austria
January 1989

89-00222

BINARY AND TERTIARY NEUTRON INDUCED REACTION CROSS SECTIONS OF CHROMIUM AND IRON

S.B. Garg
Neutron Physics Division
Bhabha Atomic Research Centre
Trombay, Bombay 400 085, India

1. Introduction

This work has been carried out under the Co-ordinated Research Programme dealing with the methods for the calculation of fast neutron nuclear data for structural materials sponsored by the International Atomic Energy Agency. The main objective of this programme is to develop and adopt nuclear models and methods for the computation of neutron induced reaction cross-sections of structural materials to be used in fission and fusion based reactor systems.

Chromium and iron are two main constituents of stainless steel which is commonly used as a structural material. In this paper investigation has been carried out for the following binary and tertiary reaction cross-sections of Cr-52 and Fe-56:

(i) (n,p), (n,pn), (n,np), (n,α), (n,nα), (n,2n) and (n,3n) cross-sections

(ii) Energy spectra of the emitted neutron, proton, α-particle and γ-rays.

(iii) Angle-energy correlated double differential cross-sections for the secondary emitted neutrons.

(iv) Total production cross-sections for neutron, hydrogen, helium and gamma-rays

The following three schemes of data evaluation have been adopted to compute the above listed cross-sections:

(a) The multistep Hauser-Feshbach (MSHF) scheme comprising optical model, statistical theory, Kalbach exciton model, Brink-Axel model of giant dipole resonances and the direct reaction model based on the distorted wave Born approximation

(b) The geometry dependent hybrid model (GDHM) scheme which makes use of the Weisskopf-Ewing evaporation model and the optical model

(c) The unified exciton model (UEM) scheme based on the master equation approach which employs Brink-Axel model for the computation of radiative capture cross-sections. Inverse cross-sections are evaluated with the appropriate optical model potential parameters for neutron, proton and alpha-particle.

Several computer codes dealing with the above stated models have been suitably modified to work on the inhorese computer. These model codes include GNASH/1/, SCAT2/2/, ELIESE3/3/, DWUCK4/4/, ALICE/85/300 /5/, and GRAPE package /6/.

2. Input Parameters

Based on the 'SPRT' method the derived neutron optical model potential parameters of Prince /7/ have been selected for Cr-52 and of Strohmaier et al /8/ for Fe-56.

Potential parameters for protons and alpha-particles have been taken from Mani /9/ and Strohmaier et al respectively.

Deformation parameters for the various discrete levels of Fe-56 have been taken from Mani for the computation of direct level excitation cross-sections. The other relevent input data for Fe-56 is contained in the paper /10/ presented at the first CRP meeting held at Bologna.

In the reaction decay chain of Cr-52, the various nuclides involved are CR-53, Cr-52, CR-51, CR-50, V-52, V-51, V-50, V-49, Ti-51, Ti-50, Ti-49, Ti-48, Ti-47, SC-48, SC-47, SC-46, Ca-45 and Ca-44.

The discrete energy levels for all these nuclides together with the gamma decay branching ratios have been taken from the literature. In the continuum energy region, level densities have been calculated with the Gilbert-Cameron /11/ formulations with the pairing energy corrections taken from Cook et al /12/. The GDHM and UEM schemes calculate level densities of composite and residual nuclides based on the back shifted Fermi gas model.

The single particle level density parameter used in the MSHF and UEM schemes is taken as A/13, A being the mass no. of the concerned nuclide. In the GDHM scheme the single particle level densities are defined as

$$g_n = N/20 \left[\frac{E_f + B_n + \epsilon}{E_f} \right]^{1/2} ;$$

$$g_p = \frac{Z}{20} \left[\frac{E_f + B_p + \epsilon}{E_f} \right]^{1/2}$$

where E_f is the Fermi-energy and ϵ is the channel energy. The other symbols have their usual meanings.

3. Results

A brief summary of results given below and contained in Figs. 1 to 16 is based on the MSHF scheme :

(i) Cr-52

(a) Fig. 1 compares the calculated and the measured secondary neutron emission spectrum at 14.1 MeV of incident neutron energy. The emission spectra of the 1st and second neutron are also shown. The interaction matrix constant K derived from this analysis is 200 MeV^3 which is kept fixed throughout the entire energy range.

(b) Calculated and measured (n, alpha) cross-sections are depicted in Fig. 2. The agreement is reasonably good indicating that the alpha-particle potential parameters employed in this study are reasonably good. Since the measurements do not exist

throughout the entire energy range, the extrapolation of these data may be taken as satisfactory.

(c) Calculated and measured (n,p) cross-sections are shown in Fig. 3. Some deviations are noted but in general the predictive capability of the model may be taken as reasonably good.

(d) Computed and measured (n,2n) cross-sections are given in Fig. 4. Agreement is quite good.

(e) Fig. 5 shows (n,p), (n,np), (n,pn), (n,alpha), (n,n alpha) and (n,2n) cross-sections. The measured data for (n,np), (n,pn) and (n,n alpha) cross-sections are almost non-existent, these consistent calculations serve to provide these data for applications.

(f) Total production cross-sections for neutron, proton, alpha-particle and gamma-rays are shown in Fig. 6. Helium is considered to be a catalyst for propagating swelling and radiation damage in stainless steel under high fluence neutron irradiation. These consistently evaluated data may serve to estimate the production of helium in such systems. Data for neutrons, protons and gamma-rays are helpful in the design of shields.

(g) Fig. 7 and 8 depict a comparison between the measured and calculated angle-energy correlated double differential cross-sections as a function of energy of the secondary emitted neutron at 60° and 120° obtained with the incident neutron energy of 14.1 MeV. The calculations have been carried out with the geometry dependent hybrid model. The areement is quite good for the low energy emitted neutrons, however some deviations are noted for the relatively high energy neutrons which are emitted in the non-compound nuclear mechanisms.

(h) The gamma-ray spectrum is shown in Fig. 9. In the low energy region, resonant behaviour is seen due to the presence of discrete levels.

(ii) Fe-56

The detailed discussion appears in ref. /10/. Only a few of the salient results obtained subsequently are described in the following :

(a) With the single level density parameter taken as A/13, the K-parameter of the averaged interaction matrix constant obtained is 400 MeV^{3}. This new value does not appreciably alter the cross-section data computed and reported earlier.

(b) With the gamma-ray competition taken correctly into account, it is noted that the radiative capture cross-section in the MeV energy region is low of the order of a few millibarns. It is also noted that with this low radiative capture cross-section the magnitude of (n,np) cross-section is affected appreciably from 5% to 80% while the other tertiary reaction cross-sections do not record any significant change.

(c) Direct level excitation cross-sections calculated with the distorted wave Born approximation are given in Fig. 10.

(d) Figs. 11, 12, 13 and 14 show the calculated and measured angle-energy correlated double differential cross-sections for

the emission of secondary neutrons at 14.1 MeV and 18 MeV at 45°, 60° and 120°. It is observed that at 14.1 MeV the calculated results at 45° and 60° are within the measured uncertainties of the data. Deviations are, however, noted in the emission of high energetic secondary neutrons at 18 MeV of incident neutron energy. These deviations may not be much of consequence in fission and fusion based reactor systems since very few neutrons will be in the energy range extending beyond 15 MeV.

(e) Calculated energy spectrum of emitted proton at 15 MeV of incident neutron energy is shown in Fig. 15 along with the experimental data. The agreement is satisfactory considering uncertainty involved in the proton potential.

(f) The calculated gamma-ray spectrum is shown in Fig. 16 at 14.1 MeV. The resonant behaviour is again noted for the low energy gamma-rays.

(h) Table 1 lists the various types of cross-sections calculated at 14.6 MeV and 25.7 MeV. This is to facilitate intercomparison of the data calculated with other evaluation schemes.

TABLE

SUMMARY OF FE-56 NEUTRON CROSS-SECTIONS INVESTIGATED UNDER THE IAEA RESEARCH CO-ORDINATED PROGRAMME WITH MULTISTEP HAUSER- FESHBACH STATISTICAL THEORY AND PRE-EQUILIBRIUM EXCITON MODEL

ENERGY	14.6 MEV	25.7 MEV
TOTAL	2507.4	2316.2
ELASTIC	1164.8	1223.2
REACTION	1342.8	1093.2
N,NX	1154.0	742.6
N,PX	147.1	274.5
N,AX	40.5	75.5
N,G	0.95	0.66
N,NG	480.7	50.0
N,2NG	600.5	430.3
N,3NG	-----	80.2
N,NPG	72.2	144.1
N,NAG	0.6	27.0
N,PG	108.5	9.8
N,PNG	38.6	240.9
N,2PG	-----	3.0
N,PAG	-----	1.2
N,P2NG	-----	27.2
N,PNPG	-----	3.4
N,AG	40.6	75.5
N,N EM	1793.0	1621.0
N,P EM	219.3	436.0
N,A EM	41.2	103.8
N,G EM	2210.0	2662.0

NOTE : THE CROSS-SECTIONS ARE GIVEN IN MILLI-BARNS A-REPRESENTS ALPHA; G-REPRESENTS GAMMA

4. Intercomparison of MSHF, GDHM and UEM Schemes of Data Evaluation

It is well known that both the geometry dependent hybrid model and the unified exciton model schemes do not account for angular momentum and parity conservation explicitly and thus the discrete levels of the composite and residual nuclides are not used in the evaluations. These schemes, thus, cannot be used for the computation of level excitation cross-sections. But these schemes are relatively simply from the computational considerations and are normally utilized in an energy region where the pre-equilibrium decay mechanism makes significant contribution to a given reaction. For neutrons, these models are generally employed at 10 MeV and above of incident energy.

An intercomparison of the three data evaluation schemes i.e. MSHF, GDHM and UEM schemes is brought out in Figs. 17 to 20 where the different types of data are depicted for Fe-56 and Cr-52 in the energy range 14.6 MeV to 24 MeV. The following salient points may be noted from these figures :

(i) The three data evaluation schemes predict total neutron emission, (n,2n) and (n,3n) cross-sections within 25% of one another. GDHM scheme being the simplest one withfewer free adjustable model parameters may be used at neutron incident energy of 14 MeV and above for quick cross-section estimates for the above noted reactions.

(ii) The charged particle emission cross-section data predicted by the three schemes differ, sometimes by factors. The estimates given by the MSHF scheme are, however, closer to the experimental data.

References

1. P.G. Young and E.D. Arthur, GNASH - A Preequilibrium Statistical Nuclear Model Code for Calculation of Cross-Sections and Emission Spectra, Report LA-6947 (1977)

2. O. Bersillon, SCAT2 - Un Programme de Modele Optique Spherique, Report CEA-N-2227 (1981)

3. S. Igarasi, Program ELIESE-3; Program for Calculation of the Nuclear Cross-Sections by Using Local and Non-Local Optical Models and Statistical Model, Report JAERI-1224 (1972)

4. P.D. Kunz, Description of the DWBA Code DWUCK4, SMR/108-2 (1984)

5. M. Blann, Code ALICE/85//300, Report UCID-20169 (1984)

6. H. Gruppelaar and J.M. Akkermans, The GRAPE Code system For The Calculation of Precompound And Compound Nuclear Reactions, Report ECN-164 (1985)

7. A Prince, Nuclear Data for Science and Technology, Antwrap Conf., 574 (1982)

8. B. Strohmaier et al, Paper Presented at the IAEA Advisory Group Meeting on Nuclear Data for Radiation Damage Assessment and Related Safety Aspects, Vienna (1981)

9. G.S. Mani, Nucl. Phys. A165, 225 (1977)

10. S.B. Garg and R.P. Anand, Neutron Induced Reaction Cross-sections of Fe-56 in the Energy Range 1 to 20 MeV, Paper Presented at the first CRP Meeting held at Bologna (1986)

11. A Gilbert and A.G.W. Cameron, Can. J. Phys. 43, 1446 (1965)

12. J.L. Cook et al., Aust. J. Phys. 20, 477 (1967)

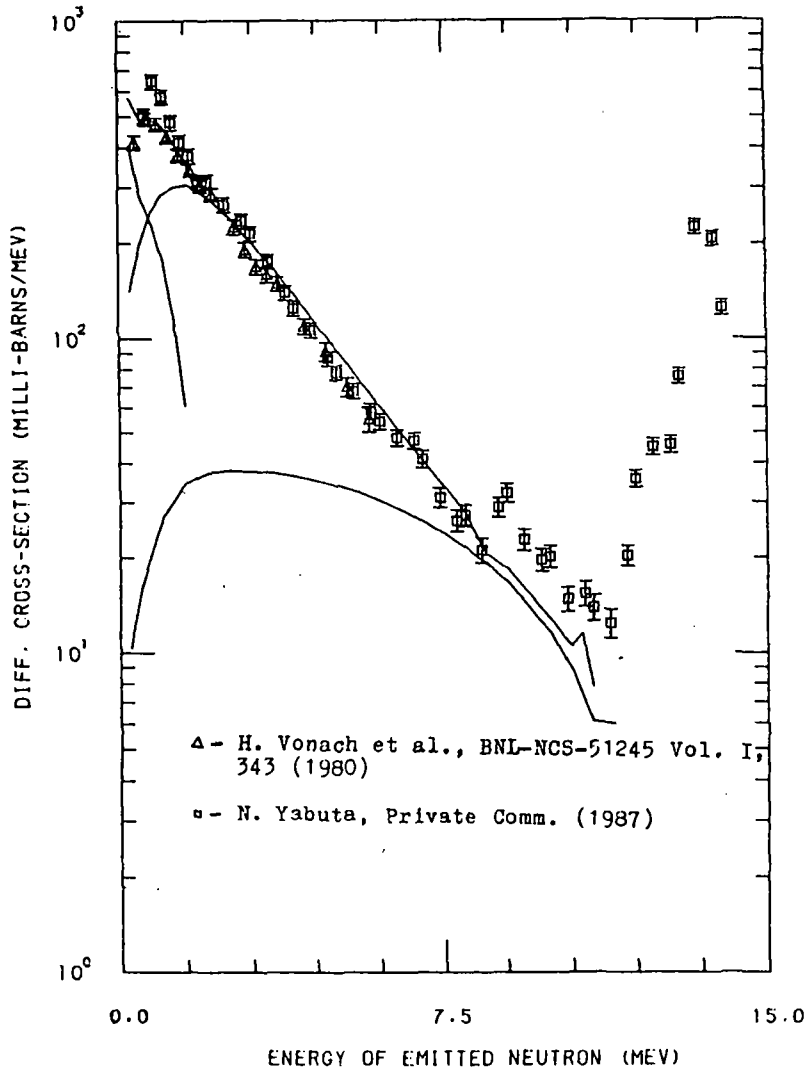

FIG. 1 : NEUTRON EMISSION SPECTRUM OF CR-52 AT 14.1 MEV

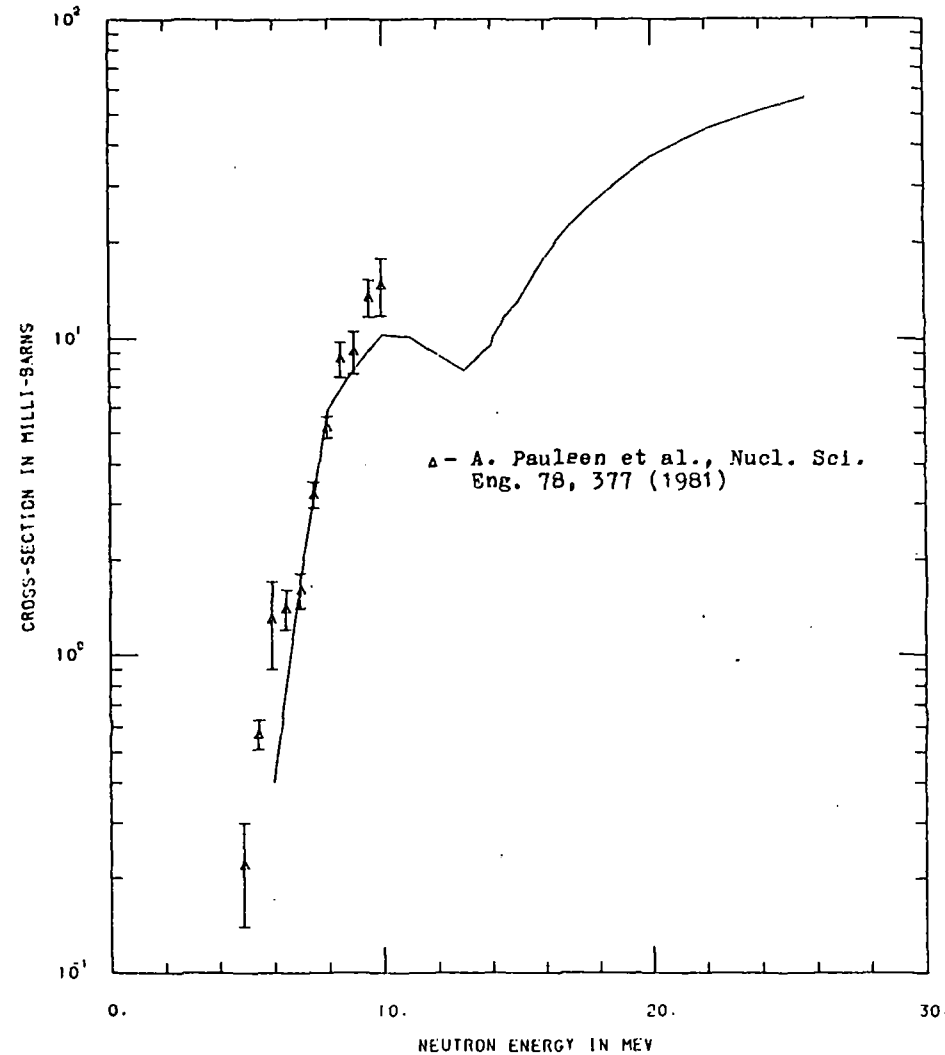

FIG2 N.ALPHA CROSS-SECTIONS OF CR-52

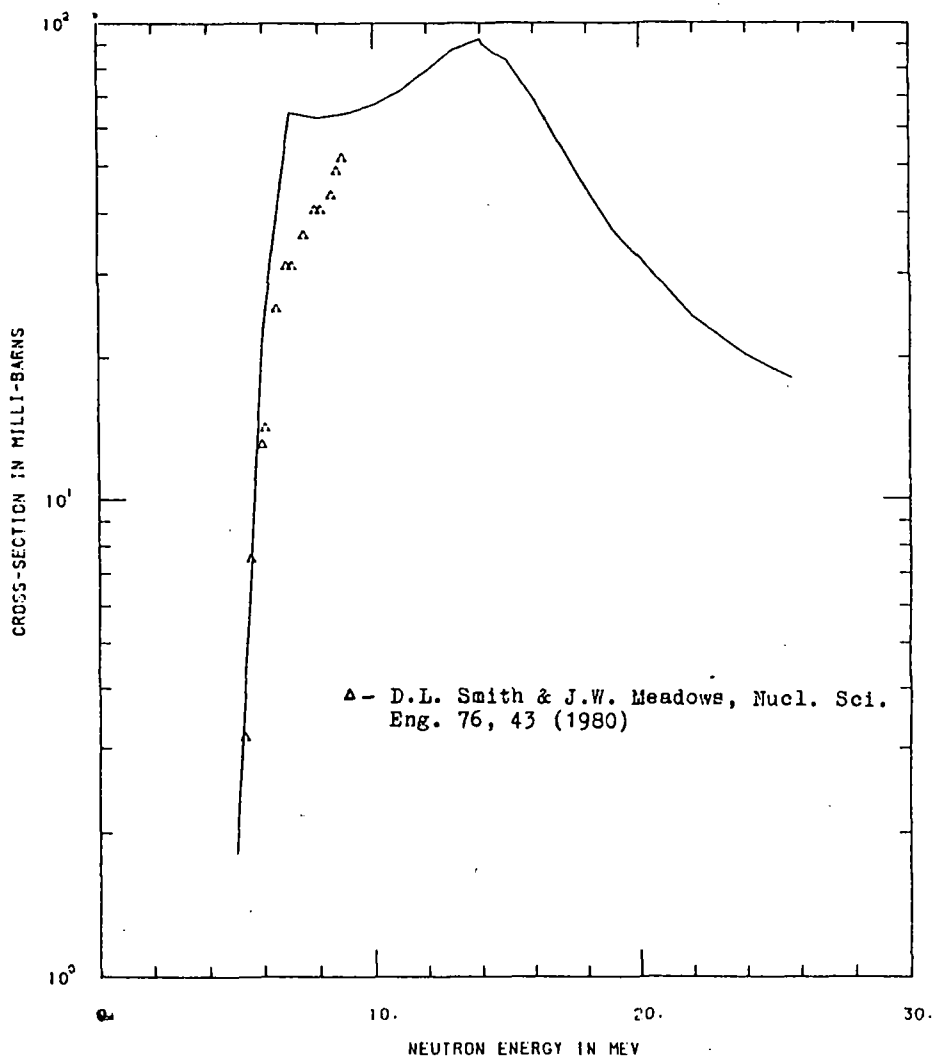

FIG3 N,P CROSS-SECTIONS OF CR-52

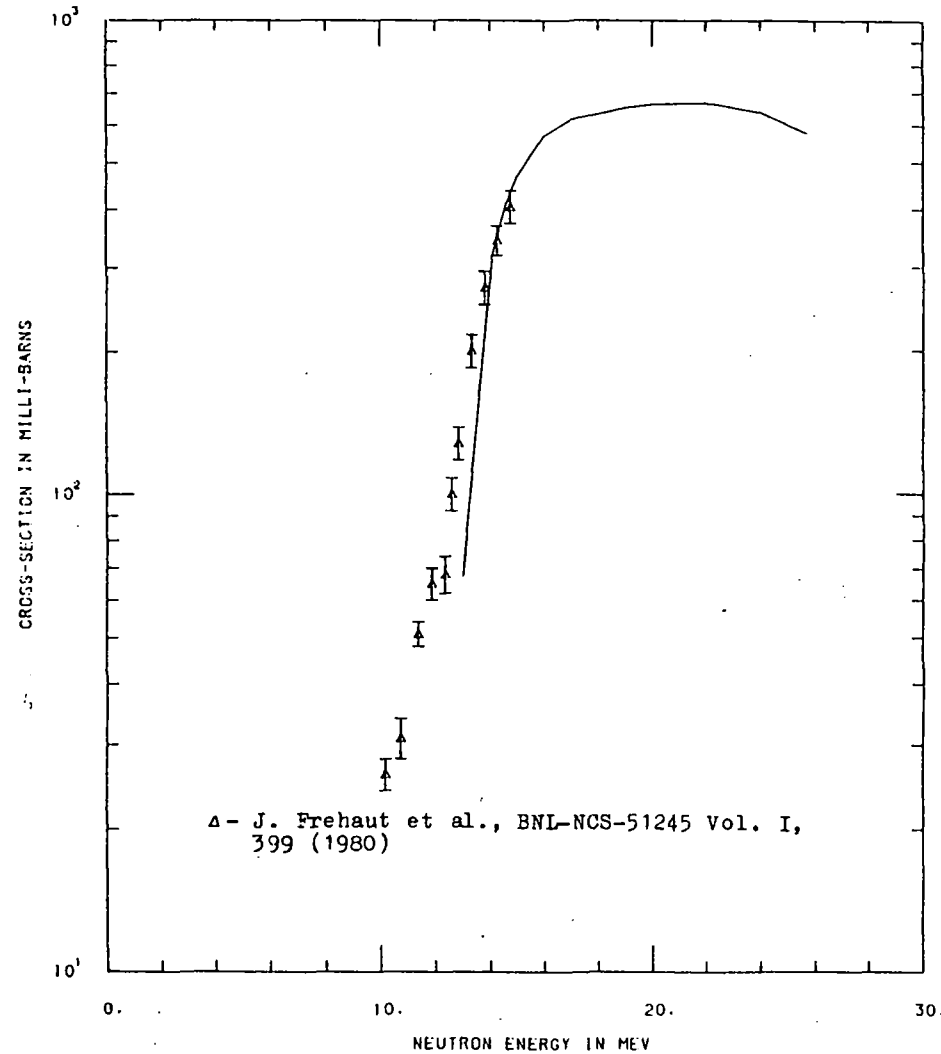

FIG4 N,2N CROSS-SECTIONS OF CR-52

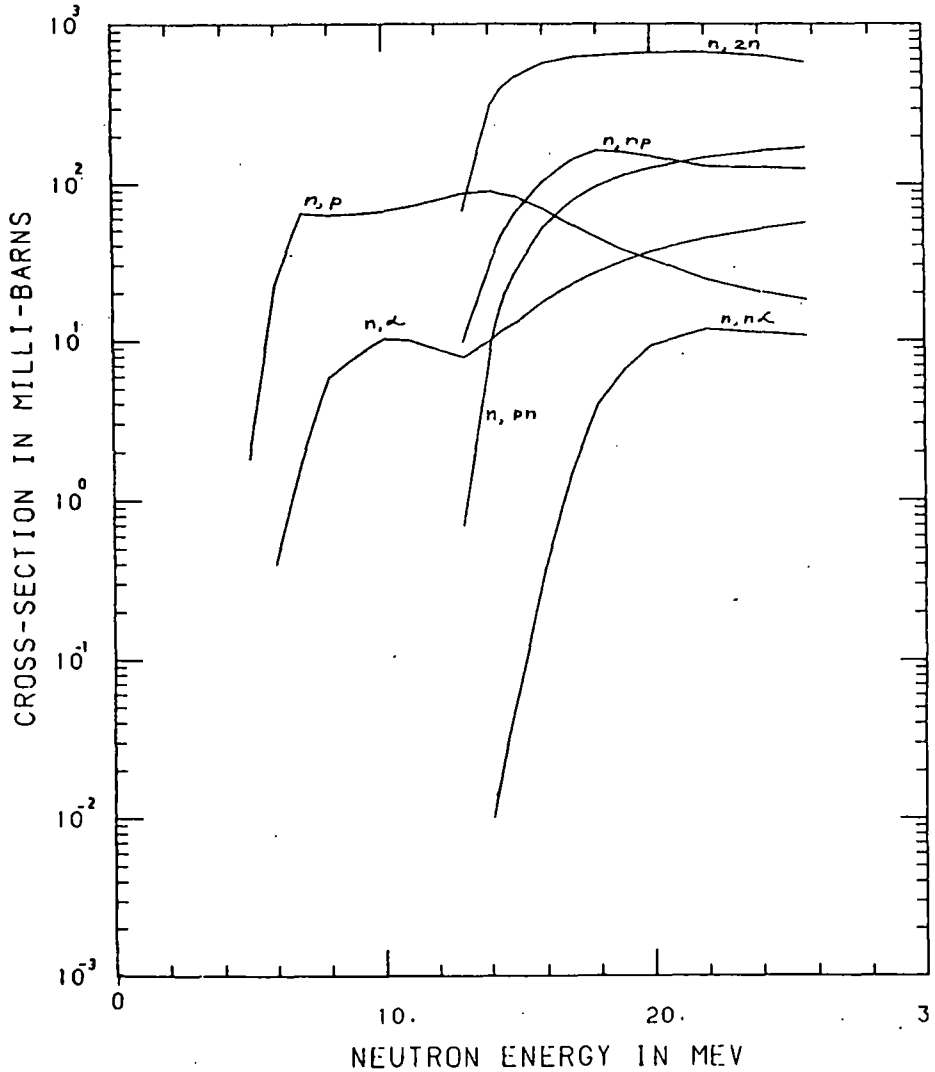

FIG. 5 N,P; N,NP; N,PN; N,ALPHA; N,N ALPHA; AND N,2N X-SECTIONS OF Cr-52

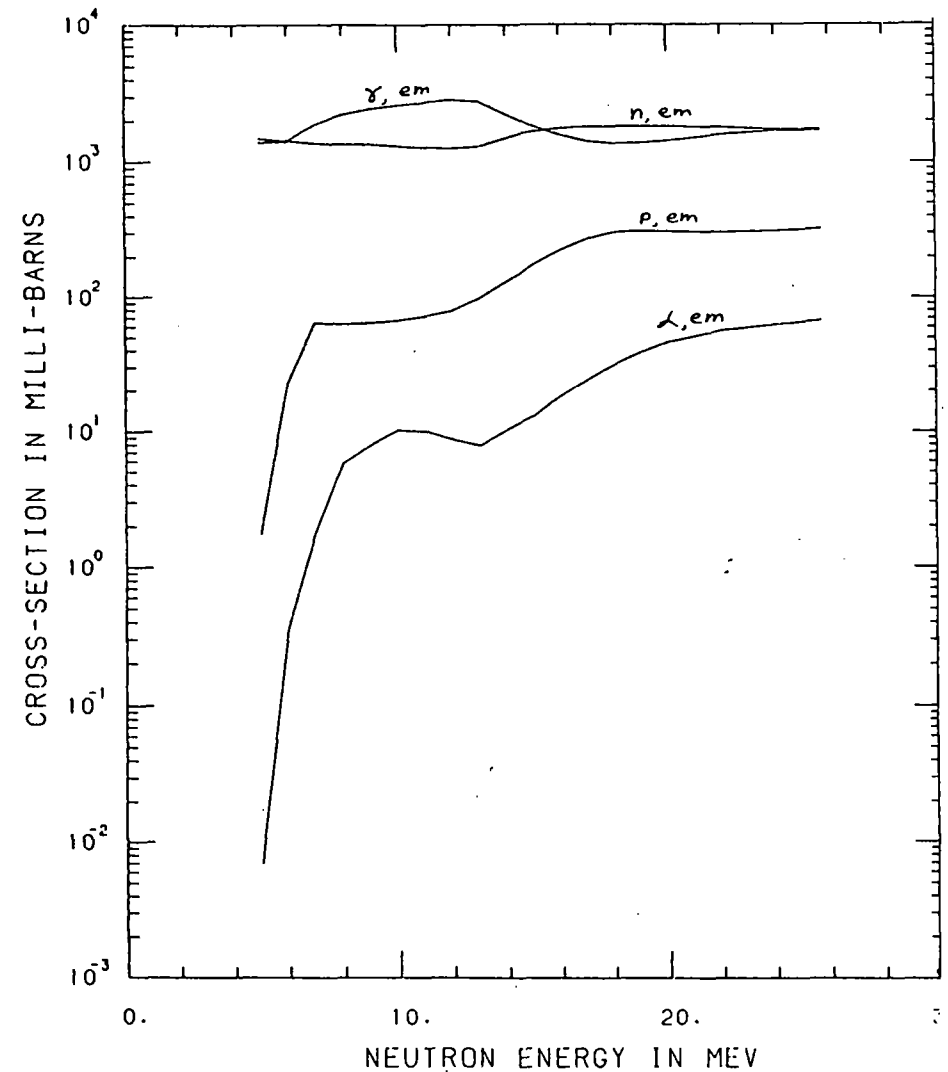

FIG. 6 N-EM., P-EM., ALPHA-EM., AND GAMMA-EM. CROSS-SECTION OF Cr-52

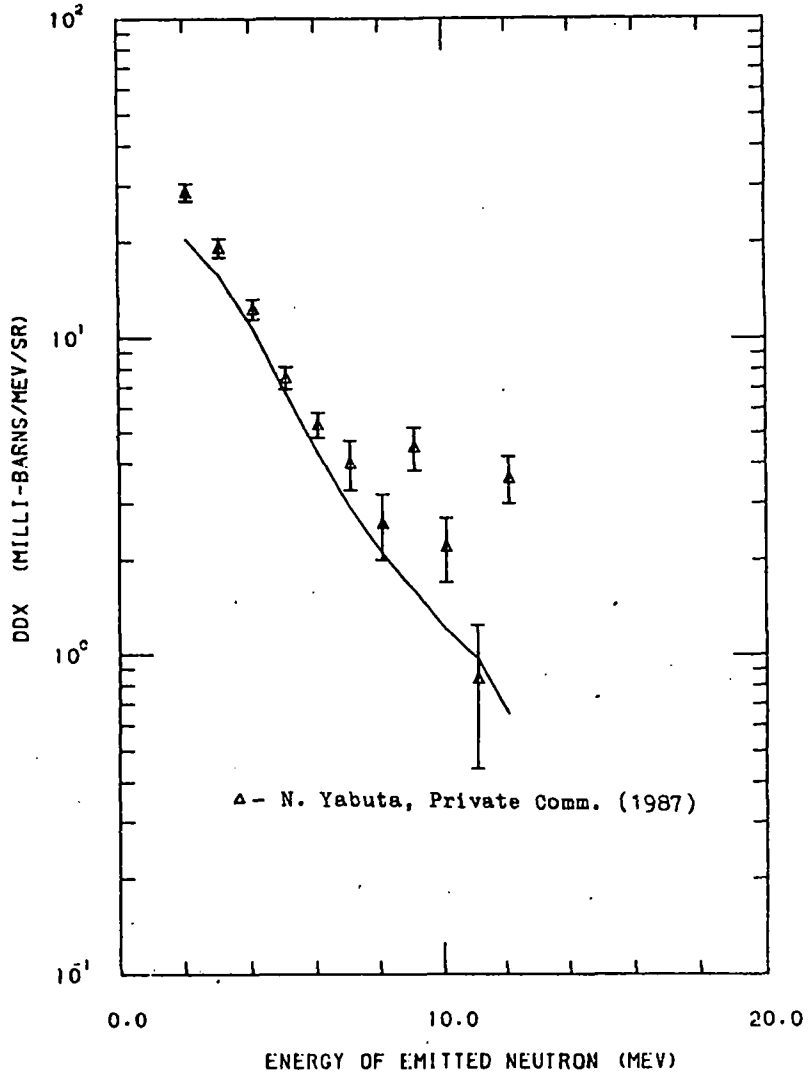

FIG. 7 : DOUBLE DIFF. CROSS-SECTION OF CR-52 AT 14.1 MEV
ANGLE = 60 DEG.

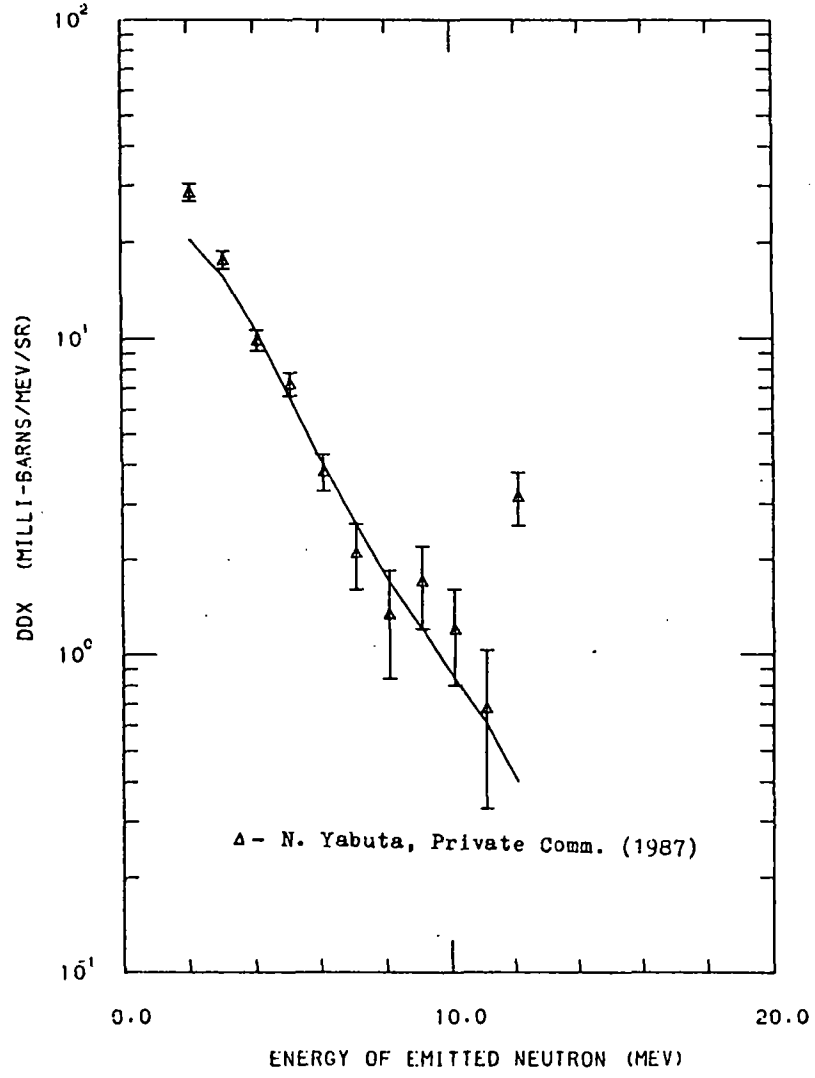

FIG. 8 : DOUBLE DIFF. CROSS-SECTION OF CR-52 AT 14.1 MEV
ANGLE = 120 DEG.

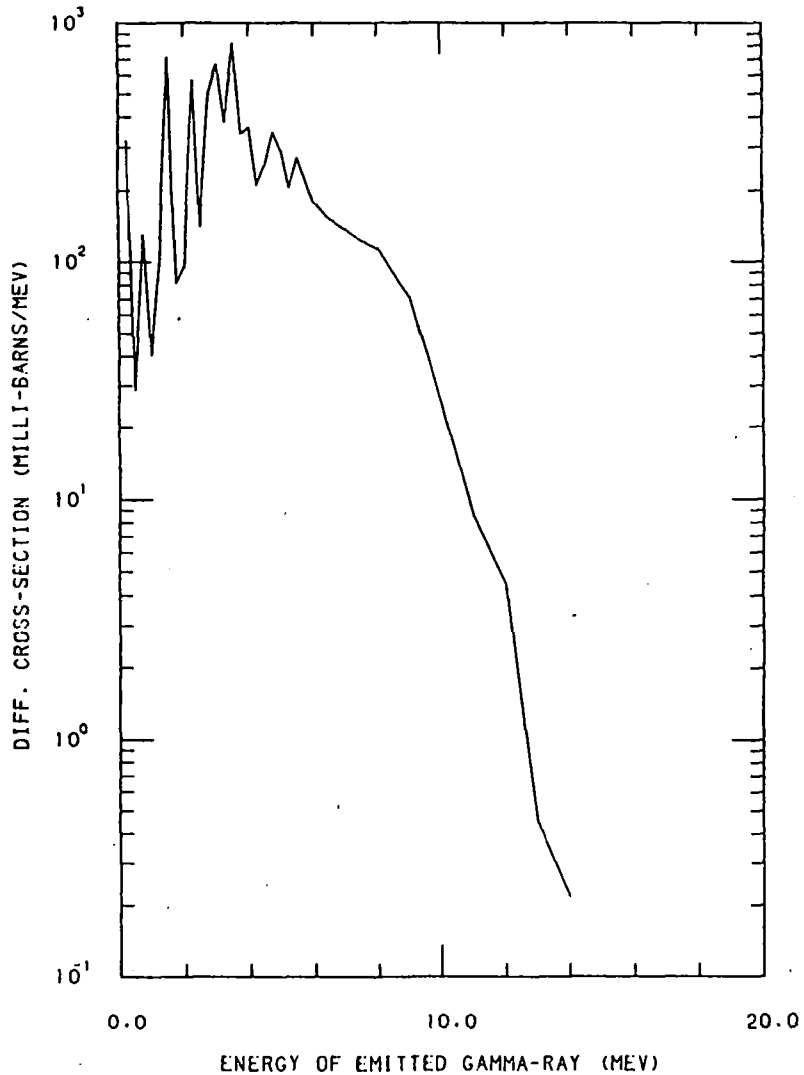

FIG. 9 : ENERGY SPECTRUM OF EMITTED GAMMA-RAYS IN CR-52

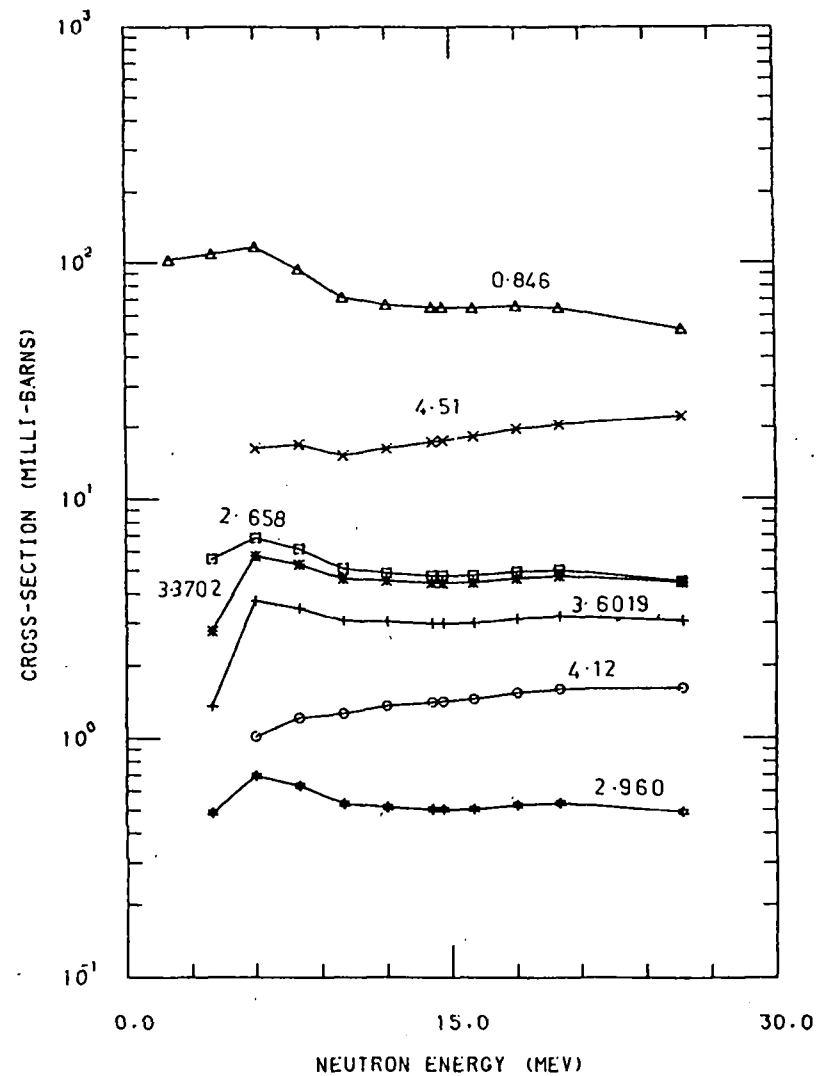

FIG.10 :DIRECT INELASTIC EXCITATION FUNCTIONS OF FE-56

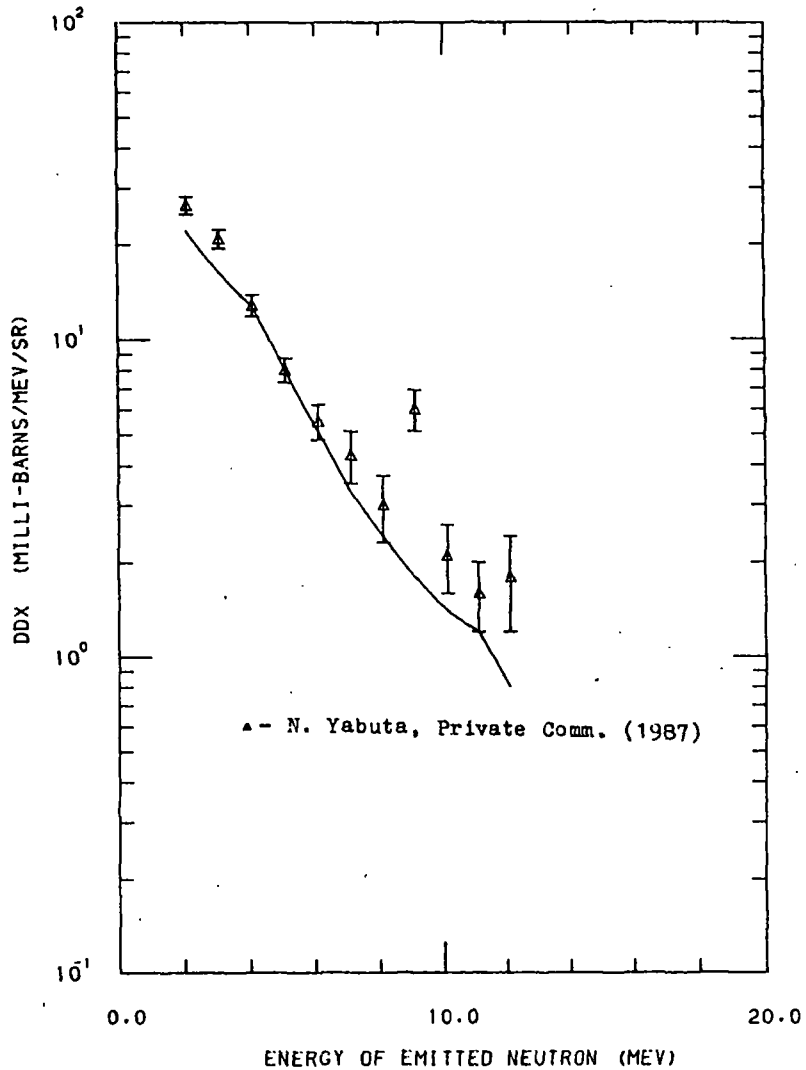

FIG. 11: DOUBLE DIFF. CROSS-SECTION OF FE-56 AT 14.1 MEV
ANGLE= 45 DEG.

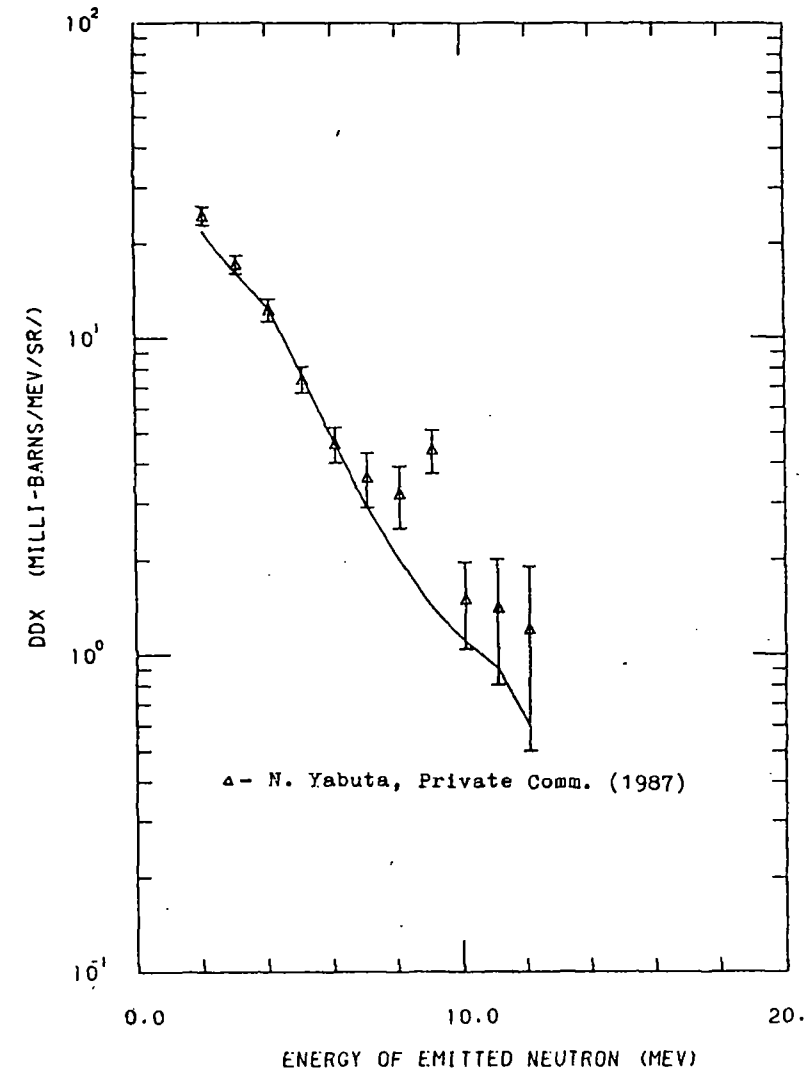

FIG. 12: DOUBLE DIFF. CROSS-SECTION OF FE-56 AT 14.1 MEV
ANGLE=60 DEG.

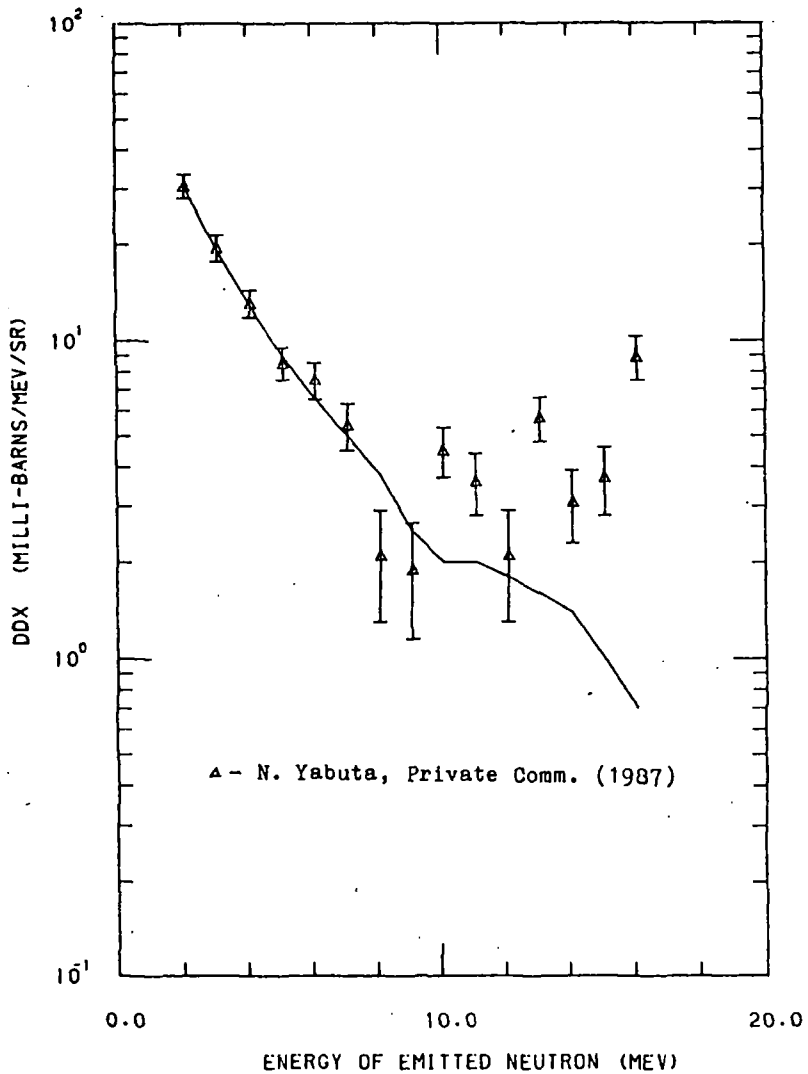

FIG. 13: DOUBLE DIFF. CROSS-SECTION OF FE-56 AT 18.0 MEV
ANGLE = 45 DEG.

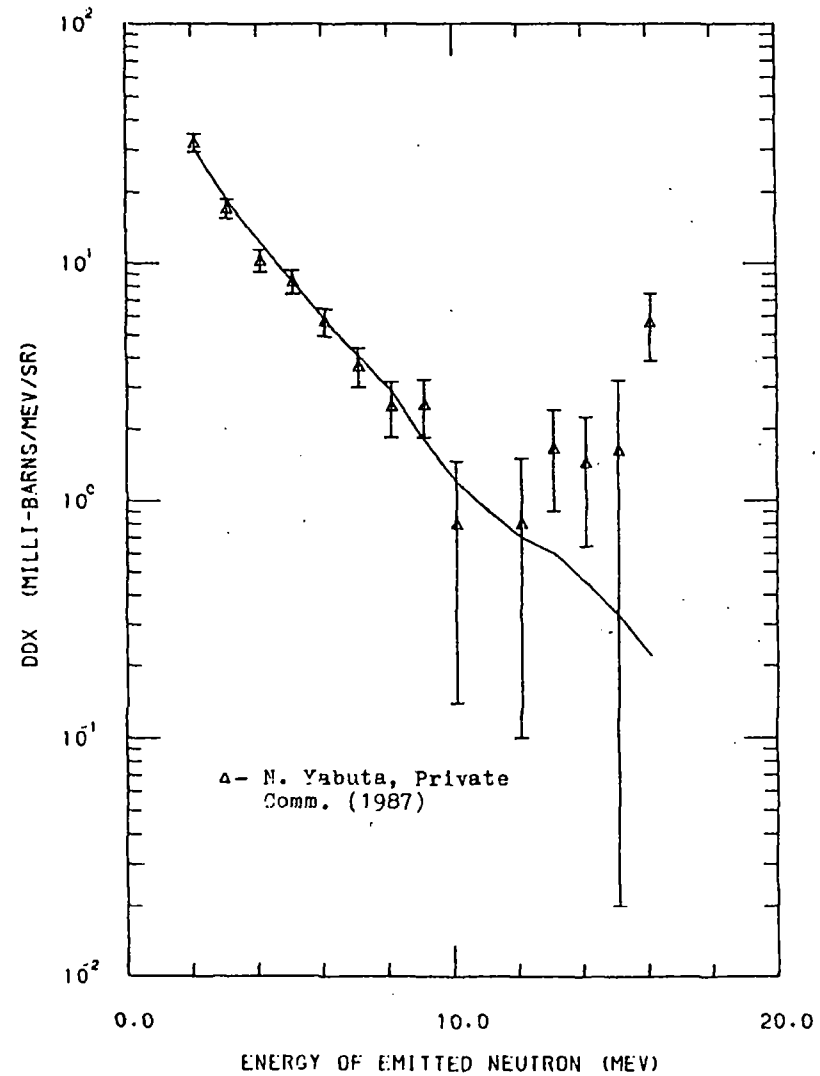

FIG. 14: DOUBLE DIFF. CROSS-SECTION OF FE-56 AT 18.0 MEV
ANGLE = 120 DEG.

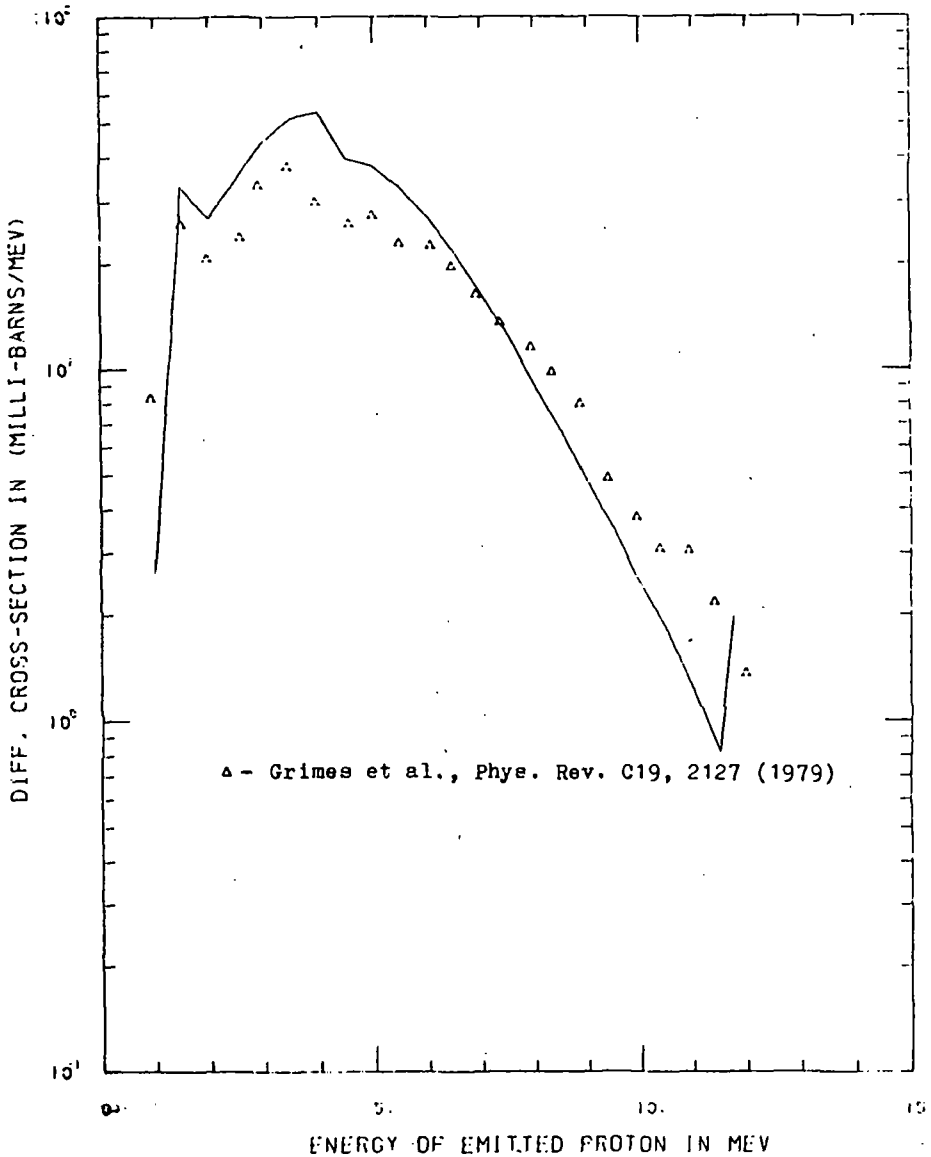

FIG.15 ENERGY SPECTRUM OF EMITTED PROTONS AT 15.0 MEV

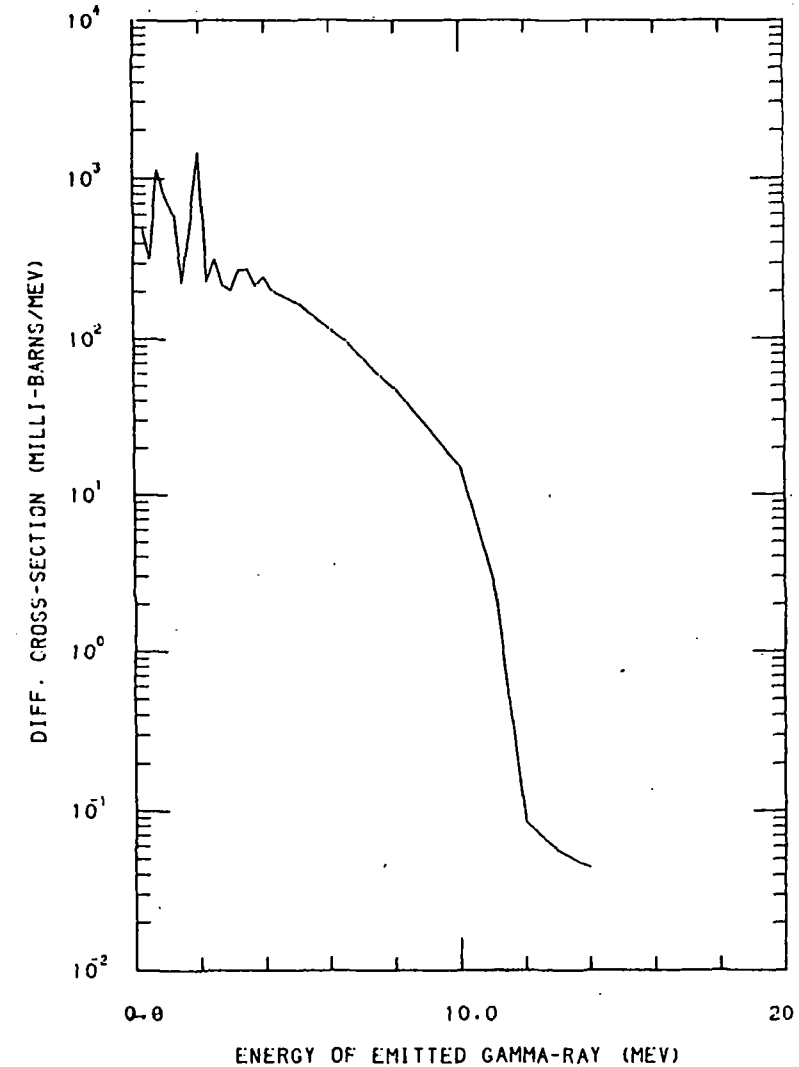

FIG. 16: ENERGY SPECTRUM OF EMITTED GAMMA-RAYS IN FE-56

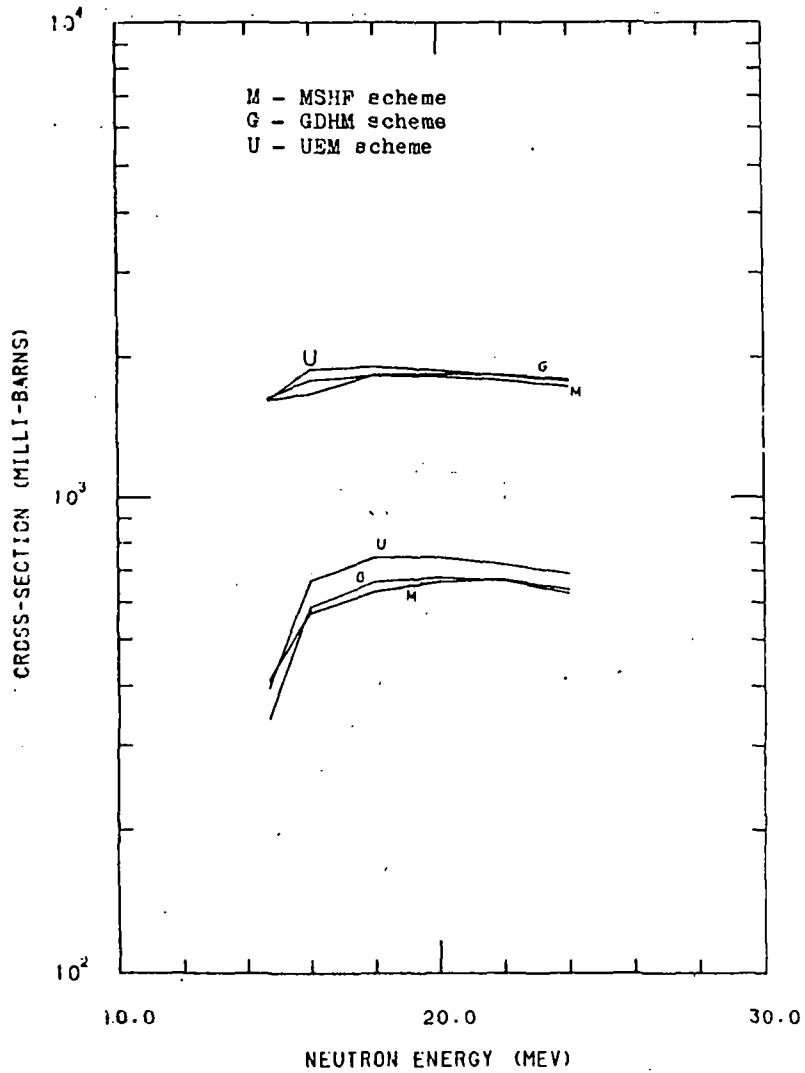

FIG. 17: INTER-COMPARISON OF NEUTRON EMISSION AND (N,2N) CROSS-SECTIONS OF CR-52 WITH MSHF,GDHM,AND UEM SCHEMES

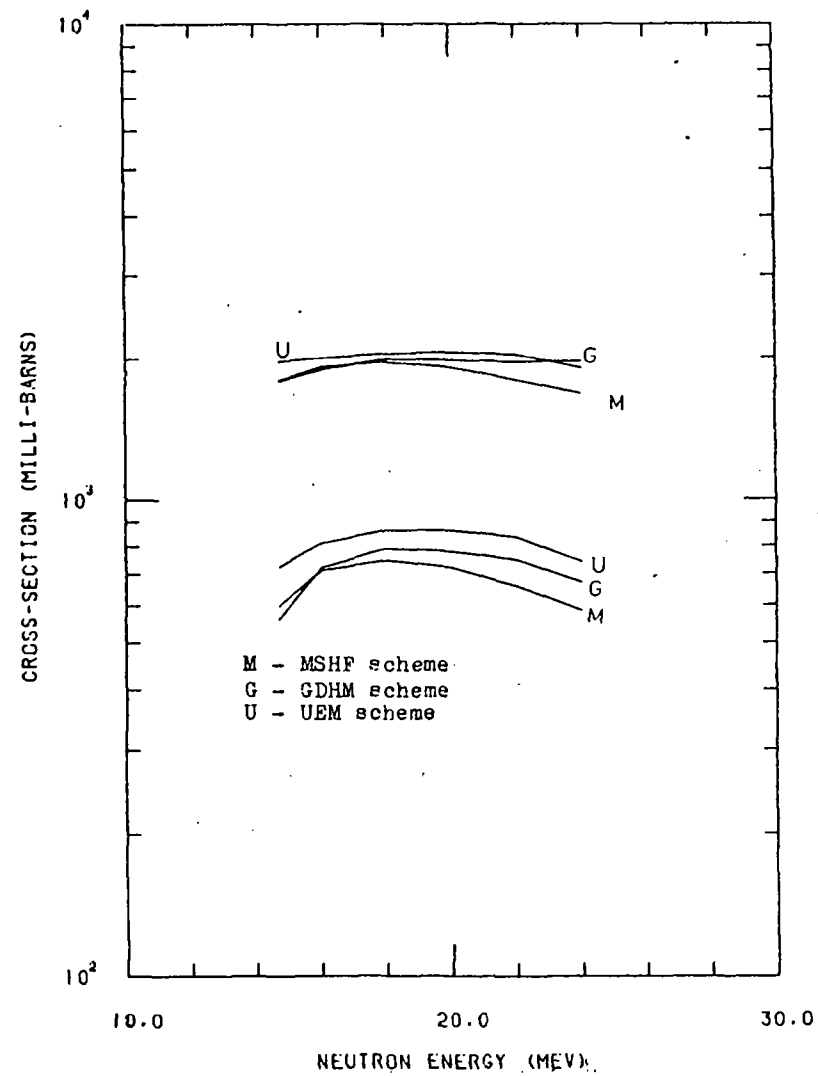

FIG. 18:

INTER-COMPARISON OF NEUTRON EMISSION AND (N,2N) CROSS-SECTIO OF FE-56 WITH MSHF,GDHM,AND UEM SCHEMES

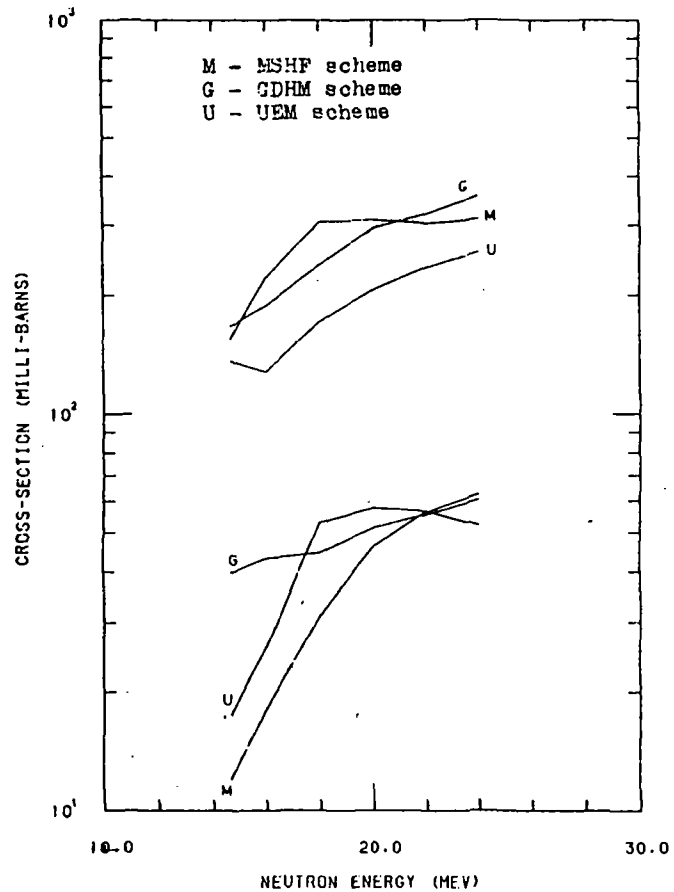

FIG. 19: INTER-COMPARISON OF PROTON AND ALPHA EMISSION CROSS-SECTIONS OF CR-52 WITH MSHF, GDHM, AND UEM SCHEMES

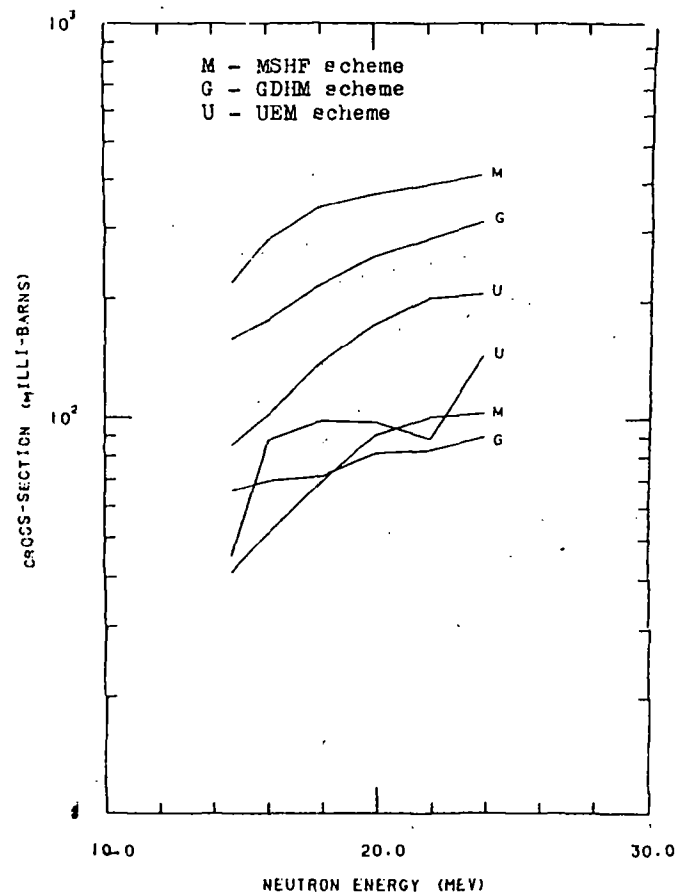

FIG. 20: INTER-COMPARISON OF PROTON AND ALPHA EMISSION CROSS-SECTIONS OF FE-56 WITH MSHF, GDHM, AND UEM SCHEMES